

# Detection of point defects upon ion irradiation by means of precipitate coherency

Z.C. Li <sup>a,\*</sup>, H. Abe <sup>b</sup>, N. Sekimura <sup>c</sup>

<sup>a</sup> *Advanced Materials Laboratory, Department of Materials Science and Engineering, Tsinghua University, Beijing 100084, China*

<sup>b</sup> *Nuclear Professional School, School of Engineering, University of Tokyo, Ibaraki 319-1188, Japan*

<sup>c</sup> *Department of Quantum Engineering and Systems Science, School of Engineering, University of Tokyo, Tokyo 113-8656, Japan*

Received 29 August 2005; accepted 28 October 2006

---

## Abstract

Transmission electron microscopy has been widely used to investigate the radiation-damage microstructures, but has limitations when observing point defects due to its resolution limit. In the present study, a dilute Cu–Co alloy, which is a typical precipitation-hardened alloy, has been selected to investigate the formation and the mobility of point defects upon ion irradiation, during which the coherent precipitates lose their coherency and exhibit incoherent strain contrast, and the coherency loss can be used to detect the point defects.

© 2006 Published by Elsevier B.V.

PACS: 28.52.Fa

---

## 1. Introduction

It is well known that ion beams interact with materials introducing change of material properties. This has been attracting attentions from both points of view of its basic understandings and applications. In order to understand the phenomena, great efforts have been performed, however, the process of the interaction and the material property change induced by ion irradiation has not yet been fully understood and still remains as a scientific issue. It is also well known that collision cascade initiated from MeV heavy ion irradiation produces highly

concentrated point defects, which can affect the micro-structural evolution [1–6] and, hence, the properties of materials including dimensional stability, changes in strength, ductility and fracture toughness, etc.

According to simple theoretical considerations, the depth of damage is expected to be comparable to the ion projected range. This relationship is normally found in semiconductors and insulators, while in some metals the observed radiation damage extends significantly deeper into the bulk, especially in those with fcc structure. The fact of the deep radiation damage of metals was mentioned by Linker et al. [7] and Sood and Dearnaley [8]. As the origin of the deep radiation damage, possible dislocation movement and atom movement mechanisms were proposed [9,10] through the observations of damage

---

\* Corresponding author.

E-mail address: [zcli@tsinghua.edu.cn](mailto:zcli@tsinghua.edu.cn) (Z.C. Li).

profiles measured by the Rutherford backscattering spectrometry. Because of its experimental limitations, lack of evidences for their proposed mechanisms was recognized. Comparatively, transmission electron microscope (TEM) has been a commonly-used and very powerful tool for investigations on the radiation-damage microstructures. Properly applied, TEM can give insights into mechanisms of damage evolution which no other technique can deliver [11]. The recent time-resolved TEM observations were successful to detect mobile defect clusters in copper and gold [3,4] and vanadium [12] under ion and electron irradiations, respectively. However, as a general understanding deducing from TEM contrast formation mechanism, for observations of those very small defects, TEM has limitations due to its resolution limit.

As a typical alloy, a Cu-base alloy has been selected to study the effects of heavy-ion irradiation on the phase stability. In the present study, by a conventional precipitation treatment [13,14], spherical coherent precipitates formed in Cu rich Cu–Co dilute alloy were used to serve as small ‘detectors’ to detect the point defects formation and mobility upon heavy ion irradiation, since the interaction between point defects and precipitates can result in the loss of precipitate coherency.

## 2. Experimental procedures

### 2.1. Specimens

Bulk of a high purity Cu–Co dilute alloy with a composition of 99%:1 wt% was obtained by melting pure copper and cobalt in an arc melt furnace with a vacuum of  $10^{-4}$  Pa at 1800 °C. The nominal impurity content of the stock material is given in Table 1.

Table 1  
Impurity analysis of Cu–1 wt%Co Ingots

Element (impurity)	Determination (wt%)
Cu	Balance
Co	1.05
Bi	<0.001
Pb	<0.001
Zn	<0.001
Cd	<0.0001
Ag	<0.001
Fe	<0.001
Te	<0.001
S	<0.002
P	<0.0003

The obtained bulk was first cold-rolled to a thickness of 0.4 mm, and then punched into disks with a diameter of 3 mm. Mechanical polishing process was conducted to obtain a pre-flat surface. To obtain the well-proportioned Co-rich precipitates, the disks after solution treatment were aged at 600 °C for 20 h. The disks were, then, electropolished for 40 s at an applied potential of 1.8 V in a solution of 80%  $H_3PO_4$  at 0 °C, so as to obtain the final flat surface. The low polishing temperature was chosen to prevent gas from being introduced into the specimens during the electrochemical process.

### 2.2. Ion irradiation

The disks were irradiated with 4 MeV  $Cu^{3+}$  ions using the High Fluence Irradiation Facility, the University of Tokyo (HIT). Self ion irradiation was performed, thus we can ignore the impurity effects introduced by incoming ions. The average flux for all samples was about  $3.3 \times 10^{15}$  ions/ $m^2$  s, with fluence ranging from  $5.4 \times 10^{16}$  to  $1.6 \times 10^{18}$  ions  $m^2$ . This corresponds to a calculated peak damage rate of  $6.0 \times 10^{-4}$  dpa s and peak damage levels of 0.01 to 0.3 dpa. Table 2 lists the irradiation conditions for this study. The vacuum during irradiation was about  $1 \times 10^{-7}$  Torr. Fig. 1 shows the depth-dependent damage profile for 4 MeV Cu ions incident on a copper target as calculated by the TRIM2003 code [15]. The maximum displacement damage occurs at a depth of about 1100 nm from the sample surface, and the total depth of the damage zone is about 1800 nm. The degree of displacement damage at the peak-damage depth is about three times greater than that at the specimen surface.

### 2.3. TEM sample preparation and observation

After irradiation, in order to reveal a wide spectrum of radiation effect, the focused ion beam (FIB) method [16] was conducted to thin the samples in cross section, such that the thin section lies parallel to the incident ion beam and contains the

Table 2  
Irradiation parameters for the ion-irradiated Cu–Co foils

Ion	Temperature (°C)	Dose (dpa)	Dose rate (dpa/s)
4 MeV $Cu^{3+}$	250, 300, 400, 500	0.01, 0.03, 0.1, 0.3	$6.0 \times 10^{-4}$

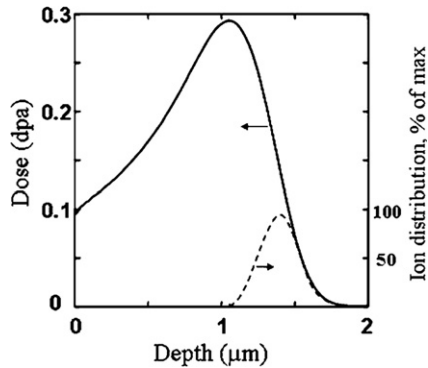


Fig. 1. Calculated 4-MeV Cu ion displacement damage profile and injected ion distribution for a copper target as determined from the TRIM 2003 code.

entire ion range. Currently, there are two techniques generally used for the FIB preparation of a cross section: the trench technique [17] and the liftout technique [18]. The main advantage of the trench technique over the liftout technique is its higher yield while the main advantage of cross-section specimens prepared using the liftout technique is that their geometry enables them to be tilted through large angles in a TEM. In the present study, we have chosen the liftout technique using an FIB system of FEI Quanta 200 3D and the preparation process can be seen in Fig. 2. Finally the specimens were examined in a JEOL 200CX electron microscope.

### 3. Results and discussion

#### 3.1. Formation of coherent precipitates

The conventional precipitation treatment typically consists of homogenizing the alloy at high temperatures, and a fast quenching process to room temperature to retain the supersaturation effectively from high temperature. The alloy is subsequently aged isothermally at a reasonably high temperature for a predetermined time to form the precipitates. In the present study, the typical precipitation-hardened alloy, Cu-1 mass%Co alloy was first solution treated at 800 °C for 5 h, and then was quenched to room temperature, followed by an aging process at 600 °C for 20 h to form the precipitates. The formed precipitates were typical of those observed in previous aging experiments on Cu–Co dilute alloys [18], i.e., spherical, coherent precipitates which nucleate homogeneously throughout the matrix, as shown in Fig. 3. According to the equilibrium phase diagram of the Cu–Co system, the composition of the precipitate is about Co–10%Cu. The lattice parameter of the precipitate is roughly 2% smaller than that of the matrix (pure copper). In the transmission electron microscopy, the strain contrast of the spherical coherent precipitate produces an elliptical image, split by a line of no contrast that is perpendicular to the reciprocal lattice vector of the particle. The mean diameter of the precipitates formed in the experiment was about 10.9 nm, and the

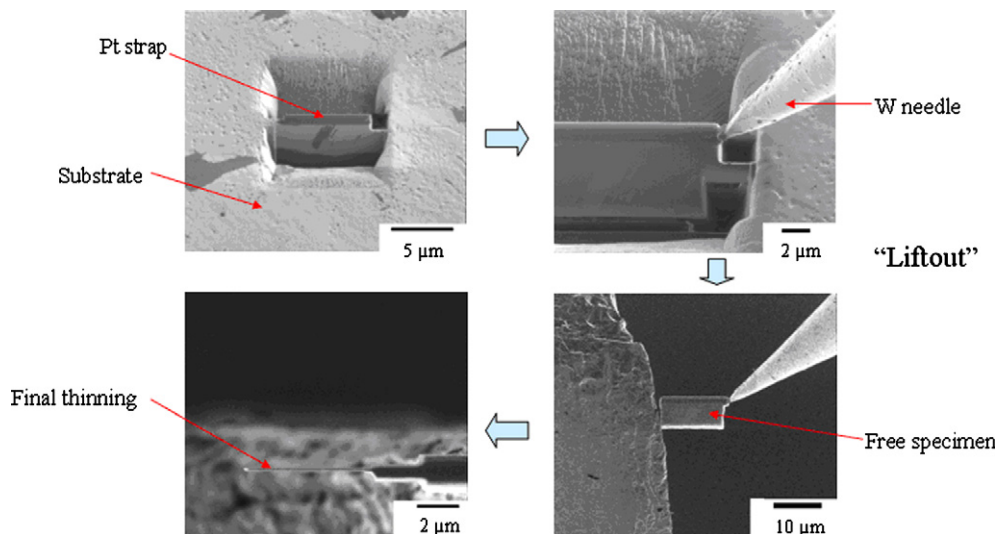


Fig. 2. Preparation process of TEM cross-section specimen by means of FIB liftout method.

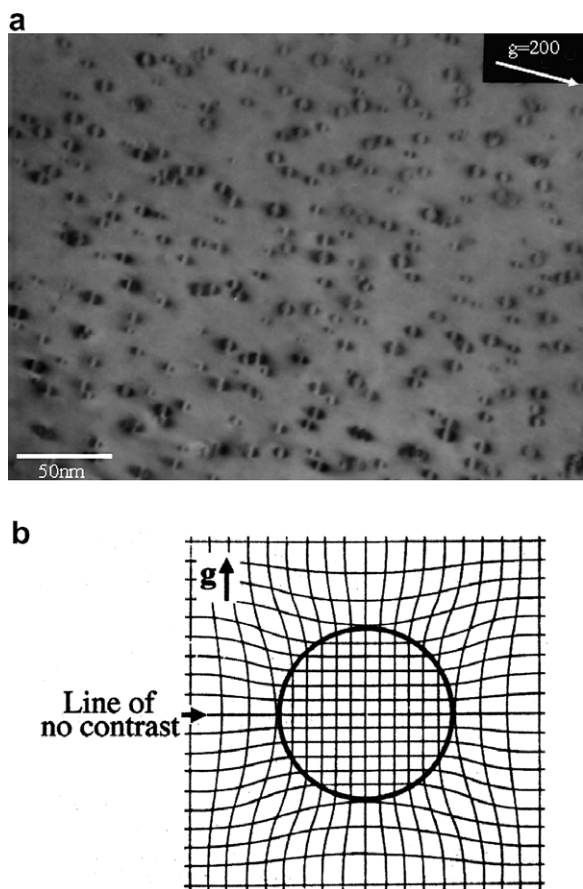


Fig. 3. (a) TEM image of Co-rich precipitates obtained after thermal treatment and (b) its schematic image.

particle number density was about  $9.1 \times 10^{15} \text{ cm}^{-3}$ , yielding a precipitate volume fraction of about 0.62%.

### 3.2. Effect of ion irradiation on coherent precipitates

It is known that in the idealized case of a coherent precipitate, the interface between the precipitates and the matrix is typified as an internal surface where constrained recombination of defect and anti-defect occurs. The interface of the coherent precipitate with the matrix is modeled as containing a distribution of saturable traps.

We can imagine that a certain volume of the parent phase (matrix) is removed and replaced by a different volume of product phase (precipitate). The difference in volume leads to a dilatational strain which is positive or negative, depending on the sign of the volume change. In the case of Cu–1%Co

dilute alloy, strain field around the coherent precipitate can be illustrated as shown in Fig. 3(b) based on the lattice parameter difference. This suggests that the strain be relieved by absorbing point defects. We presume preferential absorption of interstitials at the precipitates because distribution of vacancies locates relatively shallow comparing to that of interstitials and significant vacancy recombination prevents diffusion of vacancies beyond the end-of-range. Knoll observed dislocation segments beyond it in the same system, and concluded the coherency loss was resulted from the migration of interstitials [14], while the discussion by Fujino is similar [10]. We must mention that the assignment of point defects absorbed at the precipitates needs further study.

Transmission electron micrographs of Cu–1 wt%Co specimens irradiated at 400 °C to a peak dose of 0.3 dpa are shown in Fig. 4(b) and (c). Comparatively, Fig. 4(a) shows the micrograph of an unirradiated specimen. Comparing these TEM micrographs, one can find that the formed spherical coherent precipitates have lost their coherency upon ion irradiation, and have transformed into incoherent ones. It is known that freely-migrating point defects, generated by ion irradiation, can be absorbed at sinks, like surfaces, interfaces or grain boundaries. But in this study we employed bulk material whose grain size is much larger than the regions investigated in this work. Therefore majority of the point defects can be trapped at the precipitate–matrix interface because of their affinity in terms of lattice strain. Agglomeration of such point defects results in loss of coherency. The authors must emphasize that the loss of coherency occurs readily because it was observed even extremely low dose such as 0.01 dpa in the present study.

The depth dependence of the fraction of incoherent precipitates irradiated at 300 °C together with the depth-dependent damage profile calculated by the TRIM2003 code have been shown in Fig. 5. One can see that the coherent precipitates situated up to well beyond the end-of-range have also lost their coherency. This is resulted from the migration of free interstitials well beyond the damage zone, due to the low migration energy of Cu interstitials (about 0.2 eV). Actually, in the present study, all the observed irradiated Cu–Co specimens have lost precipitate coherency as a result of ion irradiation. Even in the low dose of 0.01 dpa, the precipitates within the damage zone have also lost their coherency. That is to say, the principal effect of ion irra-

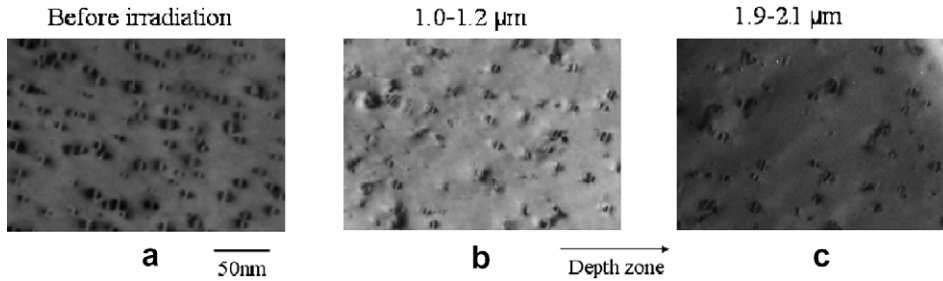


Fig. 4. TEM images of Co-rich precipitates (a) before irradiation; (b, c) after irradiation at 400 °C to a peak dose of 0.3 dpa. Incident depth ranging (b) from 1.0 to 1.2 μm and (c) from 1.9 to 2.1 μm.

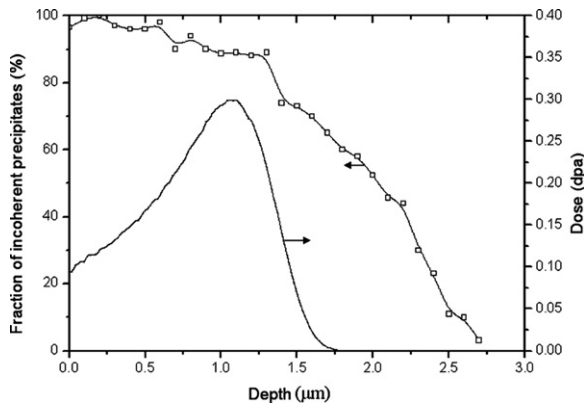


Fig. 5. Dependence of depth on the fraction of incoherent precipitates (at 300 °C).

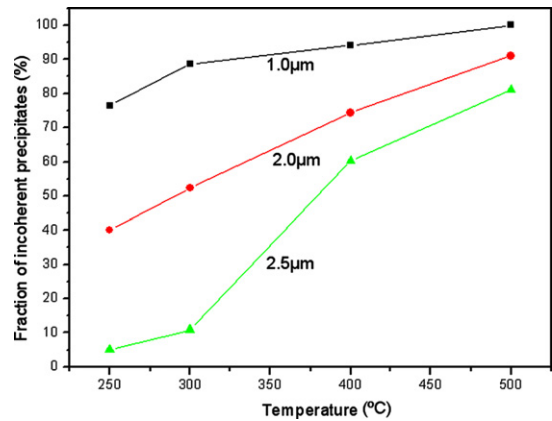


Fig. 7. Dependence of temperature on the fraction of incoherent precipitates (0.3 dpa).

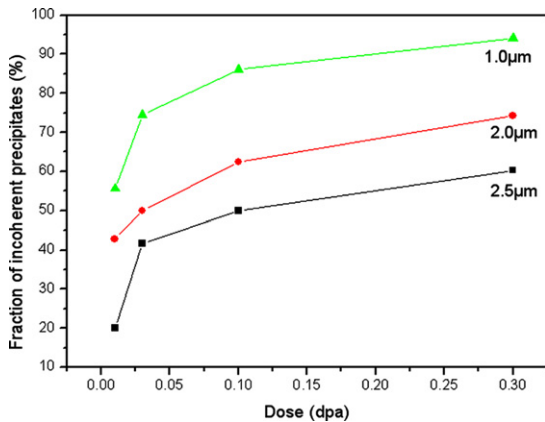


Fig. 6. Dependence of ion dose on the fraction of incoherent precipitates (at 400 °C).

diation on the coherent precipitates in Cu–Co alloy is loss of coherency.

Figs. 6 and 7 show the dose and temperature dependence of the yield of incoherency, respectively. It is clearly seen that, along depth zone, in the area near the damage peak, most coherent precipitates have changed into incoherent ones. The fraction

of incoherent precipitates increases with both ion dose and temperature. When the ion dose increases, more point defects will be produced during ion irradiation process, and the possibility of absorbing point defects by precipitate–matrix interface will be increased. And at the higher temperature the mobility of point defects will be enhanced and the possibility of trapping at precipitate–matrix interface will also be increased.

#### 4. Conclusions

Irradiation effect on the coherent precipitates formed in Cu–Co alloy is loss of coherency, which has been used to detect point defects formation and mobility during heavy ion irradiation process. Also, it is possible to use this method to investigate the behavior of defects upon lower dose irradiation.

#### Acknowledgements

This research was partially supported by the Ministry of Education, Science, Sports and Culture,

Grant-in-Aid for Scientific Research. The authors are grateful to Professor Matsumura of Kyushu University and Dr S.J. Zinkle of Oak Ridge National Laboratory, USA, for their stimulated discussion, as well as to Mr Omata and Dr Iwai of University of Tokyo for their experimental assistance.

## References

- [1] S. Ishino, T. Muroga, N. Sekimura, Nucl. Eng. Des./Fusion 2 (1985) 3.
- [2] H. Sakaida, N. Sekimura, S. Ishino, J. Nucl. Mater. 179–181 (1991) 928.
- [3] H. Abe, N. Sekimura, Y. Yang, J. Nucl. Mater. 323 (2003) 220.
- [4] H. Abe, N. Sekimura, T. Tadokoro, Mater. Trans. 46 (2005) 433.
- [5] B.X. Liu, W.S. Lai, Z.J. Zhang, Adv. Phys. 50 (4) (2001) 367.
- [6] Z.C. Li, D.P. Yu, B.X. Liu, Phys. Rev. B 65 (2002) 245403.
- [7] G. Linker, M. Gettings, O. Meyer, Ion Implantation in Semiconductors and other Materials, in: B.L. Crowder (Ed.), Plenum, New York, 1973, p. 465.
- [8] D.K. Sood, G. Dearnaley, J. Vac. Sci. Technol. 12 (1975) 463.
- [9] E. Friedland, N.G. van der Berg, O. Meyer, S. Kalbitzer, Nucl. Instrum. and Meth. B 118 (1996) 29.
- [10] Y. Fujino, Y. Igarashi, S. Nagata, Phys. Rev. B 63 (2001) 100101.
- [11] M.L. Jenkins, J. Nucl. Mater. 216 (1994) 124.
- [12] T. Hayashi, K. Fukumoto, H. Matsui, J. Nucl. Mater. 283–287 (2000) 234.
- [13] S. Matsumura, Y. Seno, Y. Tomokiyo, K. Oki, T. Eguchi, Jpn. J. Appl. Phys. 20 (1981) 605.
- [14] R.W. Knoll, PhD thesis, University of Wisconsin-Madison, 1981.
- [15] J.F. Ziegler, J.P. Biersack, U. Littmark, The Stopping and Range of Ions in Solids, Pergamon, New York, 1985.
- [16] R.M. Langford, A.K. Petford-Long, J. Vac. Sci. Technol. A 19 (5) (2001) 2186.
- [17] E. Kirk, D. Williams, H. Ahmed, Inst. Phys. Conf. Ser. 100 (1989) 501.
- [18] M.H. Overwijk, F.C. van den Heuvel, C.W.T. Bulle-Lieuwma, J. Vac. Sci. Technol. B 11 (1993) 2021.